PHYSICAL REVIEW B **69**, 224201 (2004)

# Maximum density rule for bulk terminations of quasicrystals

Z. Papadopolos*
*Institut für Theoretische Physik, Universität Tübingen, D-72076 Tübingen, Germany*

P. Pleasants
*Department of Mathematics, The University of Queensland, St. Lucia, Queensland 4072, Australia*

G. Kasner
*Institut für Theoretische Physik, Universität Magdeburg, PSF 4120, D-39016 Magdeburg, Germany*

V. Fournée
*LSG2M, CNRS UMR 7584 Ecole des Mines, Parc de Saurupt, 54042 Nancy Cedex, France*

C. J. Jenks
*Ames Laboratory, Iowa State University, Ames, Iowa 50011, USA*

J. Ledieu and R. McGrath
*Surface Science Research Centre, The University of Liverpool, Liverpool L69 3BX, United Kingdom*
(Received 7 September 2003; revised manuscript received 10 February 2004; published 8 June 2004)

Bravais' rule, of wide validity for crystals, states that their surfaces correspond to the densest planes of atoms in the bulk. Comparing a theoretical model of icosahedral Al-Pd-Mn with experimental results on sputter-annealed surfaces, we find that this correspondence breaks down, i.e., the surfaces parallel to the densest planes in the model are not necessarily the most stable bulk terminations. The correspondence is restored by recognizing that there is a contribution to the surface not just from a single geometrical plane but from a layer of stacked atoms, possibly containing more than one plane. We find that not only does the stability of high-symmetry surfaces match the density of the corresponding layerlike bulk terminations but the exact spacings between surface terraces can be determined and the typical area of the terraces can be estimated by a simple analysis of the density of layers predicted by the bulk geometric model.

DOI: 10.1103/PhysRevB.69.224201 PACS number(s): 61.44.Br, 68.35.Bs, 68.37.Ef

## I. INTRODUCTION

The tribological properties of the surfaces of quasicrystals, such as low coefficient of friction, have motivated many studies of the clean surfaces of these materials, see Ref. 1 and cited therein. These studies have led to significant progress in the past few years, especially in the case of the aluminum-based icosahedral quasicrystals. Their surfaces are shown to be perfect ''slices'' of the bulk structure, with exactly measured step heights. However, there has not been a full understanding of *which* bulk planes might be expected to be seen as surface terminations.

A rule with wide validity for crystals, first suggested by Bravais[2] and later refined by others,[3] is that ''the largest facets have the densest packing of atoms,''[4] usually interpreted as meaning that, by and large, the most stable surfaces are those parallel to the densest atomic planes in the bulk. Predictions for icosahedral quasicrystals have been calculated[5] with a modification of this rule that uses average densities of planes orthogonal to the rotational symmetry axes. Here we investigate the original Bravais rule using single planes in the context of the bulk model of Boudard *et al.*[7] for icosahedral (Al-Pd-Mn) [(i-AlPdMn)] and notice that the rule does not hold in this form, since the *densest planes* are orthogonal to the twofold axes but it has been observed[6] that the *most stable surfaces* are orthogonal to the fivefold axes. Consequently, for quasicrystals we propose modifying the rule to use densities of thin layers of bulk planes instead of densities of single bulk planes. This is suggested by the fact that, whereas the distances between neighboring high-density planes in the bulk of an ordinary crystal are 1.5–2.0 Å, in the geometric bulk model[1,8–10] $\mathcal{M}$ of $F$ phase[11] icosahedral quasicrystals the distances are 0.2–1.5 Å. Because the radius of an Al atom is 1.18 Å (Ref. 12) and the bulk terminations (at least the fivefold ones) are rich in aluminum,[13] we consider a thin layer of 2–3 planes of stacked atoms as a single termination. We estimate by inspection of i-AlPdMn that the distance $\delta$ between the atomic centers of neighboring planes, if they are to be regarded as in the same thin layer, must be less than some $\delta_{max}$ in a range 0.53–0.86 Å, but significantly less than 0.86 Å. We show that the observed surface structure of i-AlPdMn is consistent with this modified rule. Measurements of the fivefold surfaces of i-AlCuFe are also consistent with this new rule. Preliminary investigations of a scanning tunneling microscopy (STM) image of a decagonal plane of decagonal Al-Cu-Co,[14] based on Burkov's model,[15] indicate that dense atomic layers, rather than dense planes, are relevant for decagonal quasicrystals as well.[16]

## II. EXPERIMENTAL EVIDENCE ON THE STABILITY OF SURFACES OF ICOSAHEDRAL Al-Pd-Mn

We first present experimental evidence on the stability and texture of sputter-annealed surfaces of i-AlPdMn derived

 

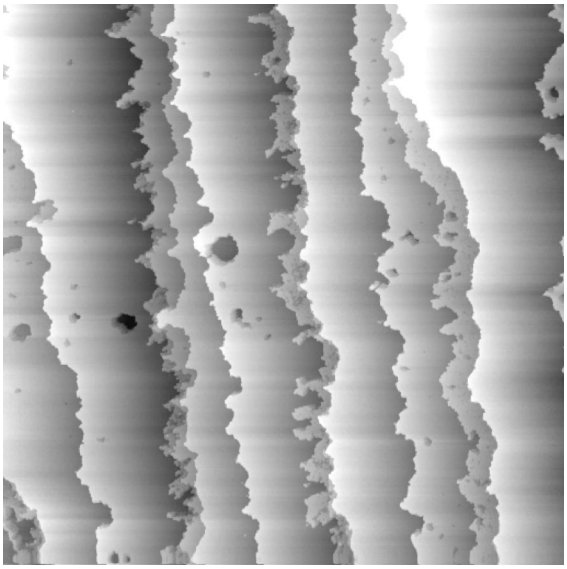

FIG. 1. STM image of a fivefold surface of i-AlPdMn, size $1750\times1750$ nm$^2$. Large scale terraces appear.

from STM and low-energy electron diffraction (LEED) measurements.

Our STM images of the fivefold surfaces of i-AlPdMn (Fig. 1) reveal large scale terraces[1] that are stable after Ref. 6. We showed[9] that the intervals between terraces on the fivefold surfaces of i-AlPdMn match a Fibonacci sequence of planes in the model $\mathcal{M}$ with $S=4.08$ Å and $L=\tau S=6.60$ Å, where $\tau=(1+\sqrt{5})/2$. In Refs. 1 and 13 it was found that the fivefold bulk terminations of i-AlPdMn consist of two close atomic planes. In Ref. 1 the separation between the planes is given as 0.48 Å in the bulk, which contracts to a separation of 0.38 Å at the real surface.[13]

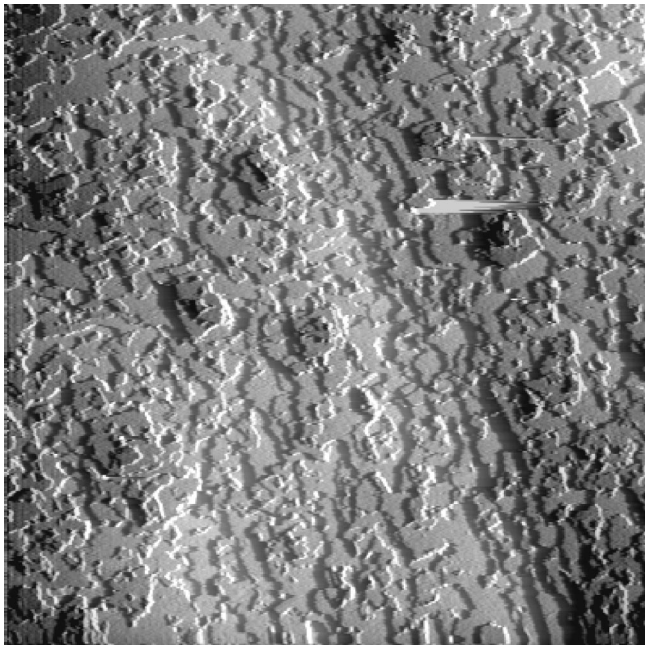

FIG. 2. STM image of a twofold surface of i-AlPdMn, size $2000\times2000$ nm$^2$. Terraces appear, but not in a clear sequence on a large scale. At the scale of the image the picture looks rather like a landscape with mesas and flat depressions.

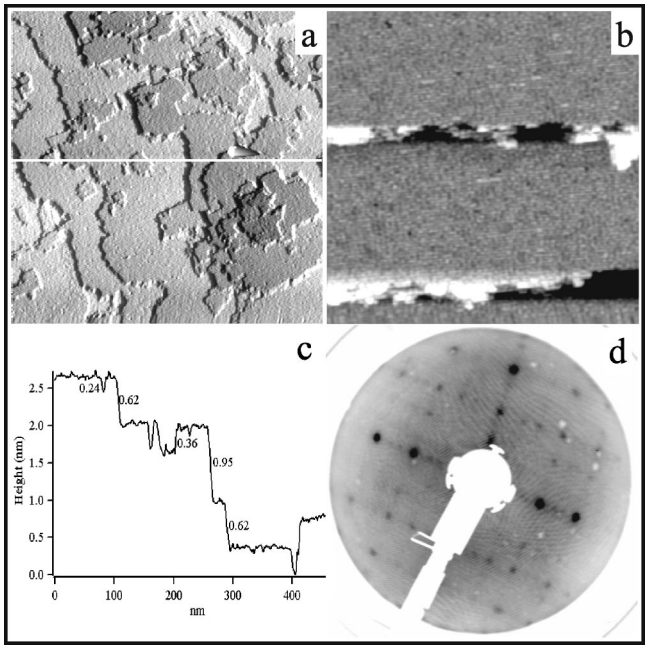


FIG. 3. (a) STM image of a twofold terrace-stepped surface of i-AlPdMn, size $500\times500$ nm$^2$. Small scale terraces and depressions appear. (b) Flattened image covering only three terraces and two steps, size $160\times160$ nm$^2$. (c) Height profile along the line in (a) with step heights. Note the large terraces with heights 0.62 nm and 0.95 nm on which are superimposed smaller terraces with heights 0.24 nm and 0.36 nm. (d) LEED pattern at 50 eV.

According to Ref. 6 both twofold and threefold surfaces *facet*, i.e., they are less stable.

Terraces are also seen on the twofold surfaces of i-AlPdMn, but they are not so pronounced as those on fivefold and threefold surfaces. The twofold terraces are broken up by holes and lumps which can be interpreted as fragments of intermediate, less stable terraces; see Figs. 2 and 3(a)–3(c). The heights of the large terraces and depths of the holes have been measured, see Figs. 3(a) and 3(c).

The threefold surfaces of i-AlPdMn show clear medium scale terraces with only few flat holes and lumps; see Fig. 4.

Also the sizes of the facets of the equilibrium shape of grown-in voids in Fig. 1(a) of Ref. 17 indicate that for i-AlPdMn the fivefold surfaces are the most stable, followed by twofold and threefold surfaces.

Further evidence that the traditional Bravais rule is broken for quasicrystals comes from the high-resolution STM image of a particularly clear and stable fivefold surface of i-AlPdMn in Fig. 4 of Ref. 18. The Al atoms in the single terminating plane are clearly distinguished and can be counted. It is easy to estimate the resulting atomic density of the plane. It is smaller than the maximal density of fivefold planes in the model $\mathcal{M}$, which is 0.086 Å$^{-2}$; see Table II.

### III. BRAVAIS' RULE FOR QUASICRYSTALS

We explain the experimental evidence cited above in terms of the particular geometric model[1,8–10] $\mathcal{M}$ of the qua-

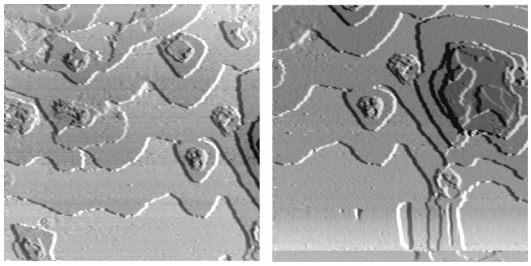

FIG. 4. Two STM images of a threefold surface of i-AlPdMn, each $800\times800$ nm$^2$. These images overlap, with a common part that can be easily recognized. There are clear terraces of medium area (smaller than in the fivefold case). Flat depressions and lumps appear on the terraces.

sicrystals i-AlPdMn (Refs. 7 and 19) and i-AlCuFe.[19,20] The model is a superposition of three icosahedral quasilattices $q$, $a$, and $b$ of atomic positions in the physical space $\mathbb{E}_\parallel$. These are defined in the caption to Table I. As described in Ref. 1 and references cited therein, there is a *coding space* $\mathbb{E}_\perp$, containing three *windows* $W_q$, $W_a$, and $W_b$ (shown in Fig. 5, see also Fig. 8 of Ref. 10) and a $*$-*map* (effected by changing $\tau$ to $-1/\tau$ everywhere[21]) that takes each point of one of the quasilattices into a point of the module $M_F$ in the corresponding window. Conversely (also under the $*$-map), the module points in the windows give rise to all the atomic positions and *define* the model $\mathcal{M}$. The $*$-map is not continuous: it maps a discrete unbounded quasilattice to a dense point set bounded by a window. It does, however, map lines and planes in physical space $\mathbb{E}_\parallel$ to lines and planes in coding space $\mathbb{E}_\perp$ and preserves orthogonality. It is also reversible from $\mathbb{E}_\perp$ to $\mathbb{E}_\parallel$. The atomic positions on a given plane $P$, orthogonal to a chosen axis $z_\parallel$ (fivefold, threefold, or twofold) along $z_\parallel$, belong to a given class $h$ ($=q$, $a$, or $b$) arise as the inverse images under the $*$-map of the points of $M_F$ in the intersection of the window $W_h$ with the image plane $P*$,

TABLE I. The atomic positions $x=\frac{1}{2}(n_1,\ldots,n_6)$ in any fivefold or threefold plane are all of the same class, but twofold planes may contain atomic positions of all classes. A unit normal vector to an $i$fold plane ($i=5$, 3, or 2) is denoted by $n_\parallel^i$. The symbol $e$ stands for an even integer and $o$ for an odd one. The scalar products are given in the units $\kappa_3=③/3$, $\kappa_5=⑤/\sqrt{5}$, and $\kappa_2=②/4$, where $⑤/\sqrt{\tau+2}=③/\sqrt{3}=②/2=1/\sqrt{2(\tau+2)}$. We use a fivefold coordinate system of six unit orthogonal basis vectors projected icosahedrally. (Some authors working with similar models use a threefold coordinate system, Ref. 8.)

| Class criterion | Class | $n_\parallel^3 x_\parallel[\kappa_3]$ | $n_\parallel^5 x_\parallel[\kappa_5]$ | $n_\parallel^2 x_\parallel[\kappa_2]$ |
|---|---|---|---|---|
| $\frac{1}{2}(e_1,\ldots,e_6)$; $\frac{1}{2}\Sigma_i e_i=e$ | $q_{D_6}$ | $e+e\tau$ | $e+e\tau$ | $e+e\tau$ |
| $\frac{1}{2}(e_1,\ldots,e_6)$; $\frac{1}{2}\Sigma_i e_i=o$ | $b$ | $o+o\tau$ | $o+e\tau$ | $e+e\tau$ |
| $\frac{1}{2}(o_1,\ldots,o_6)$; $\frac{1}{2}\Sigma_i o_i=o$ | $a$ | $o+e\tau$ | $e+o\tau$ | $e+e\tau$ |
| $\frac{1}{2}(o_1,\ldots,o_6)$; $\frac{1}{2}\Sigma_i o_i=e$ | $c$ | $e+o\tau$ | $o+o\tau$ | $e+e\tau$ |

which is orthogonal to $z_\perp$ in $\mathbb{E}_\perp$ (see Ref. 9 and, in particular, Fig. 12 in Ref. 1). It turns out that the atomic density function $\rho(z_\parallel)$ of planes orthogonal to a given axis $z_\parallel$, which is an erratic discrete function on the physical space axis $z_\parallel$, is a continuous function [which we also designate $\rho(z_\perp)$] on the coding space axis $z_\perp$ and can be graphed as in Figs. 6, 7, 9, and 10. Hence the atomic densities of terminations are most conveniently calculated and visualized in $\mathbb{E}_\perp$.

To specify scale in the model $\mathcal{M}$ we use standard distances, denoted by ⑤, ②, and ③ along the fivefold, twofold, and threefold axes, respectively, which are related by $③/\sqrt{3}=⑤/\sqrt{\tau+2}=②/2[=1/\sqrt{2(\tau+2)}]$, where $\tau=(1+\sqrt{5})/2$. The standard distances are used both in the observable space $\mathbb{E}_\parallel$ and in the coding space $\mathbb{E}_\perp$. The standard distance ⑤ ($=1/\sqrt{2}$) in $\mathbb{E}_\parallel$ is set to be 4.561 Å for i-AlPdMn and 4.465 Å for i-AlCuFe.

For ordinary lattices the density of points in a plane depends only on the orientation of the plane, but the density of a plane section of the quasilattices $q$, $a$, and $b$ is a product of two factors: the *module factor*[22] that depends on the orientation of the plane (see row 8 in Table II and cf. Table III of Ref. 5) and the *window factor* that is the area of the section of the window by the $*$-mapped plane in coding space. We also use the fact that each plane orthogonal to a threefold or fivefold axis contains points of one quasilattice $q$, $a$, or $b$ only, but each plane orthogonal to a twofold axis may contain points of all three quasilattices, as shown in Table I.

Row 9 of Table II gives the maximum density of planes in the main symmetry directions, and rows 10 and 11 the maximum density of terminations (described below). As in the

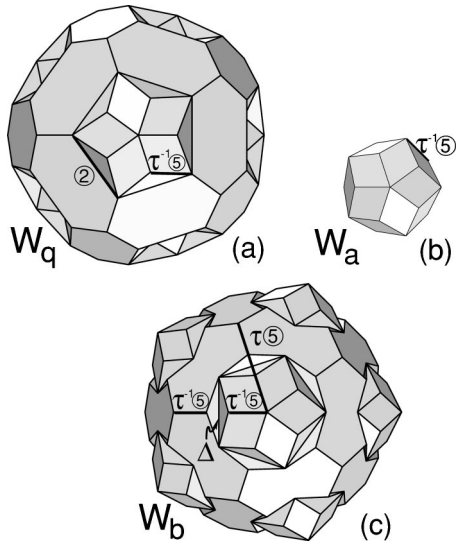


FIG. 5. The windows $W_q$, $W_a$, and $W_b$ are polyhedra in the coding space $\mathbb{E}_\perp$. They define the geometric model $\mathcal{M}$ of atomic positions based on the icosahedral $D_6$ module $M_F$. The model $\mathcal{M}$ describes both i-AlPdMn and i-AlCuFe. (a) $W_q$ with edge lengths $\tau^{-1}$ ⑤ and ② $=2⑤/\sqrt{\tau+2}$. (b) $W_a$ is a triacontahedron of edge length $\tau^{-1}$⑤. (c) $W_b$ is obtained by taking the marked tetrahedra ($\Delta$) away from the triacontahedron of edge length $\tau$⑤. The tetrahedron $\Delta$ has two mirror symmetry planes and edges of lengths $\tau^{-1}$⑤, $\tau^{-2}$⑤, and ②. The windows fulfill the closeness condition.

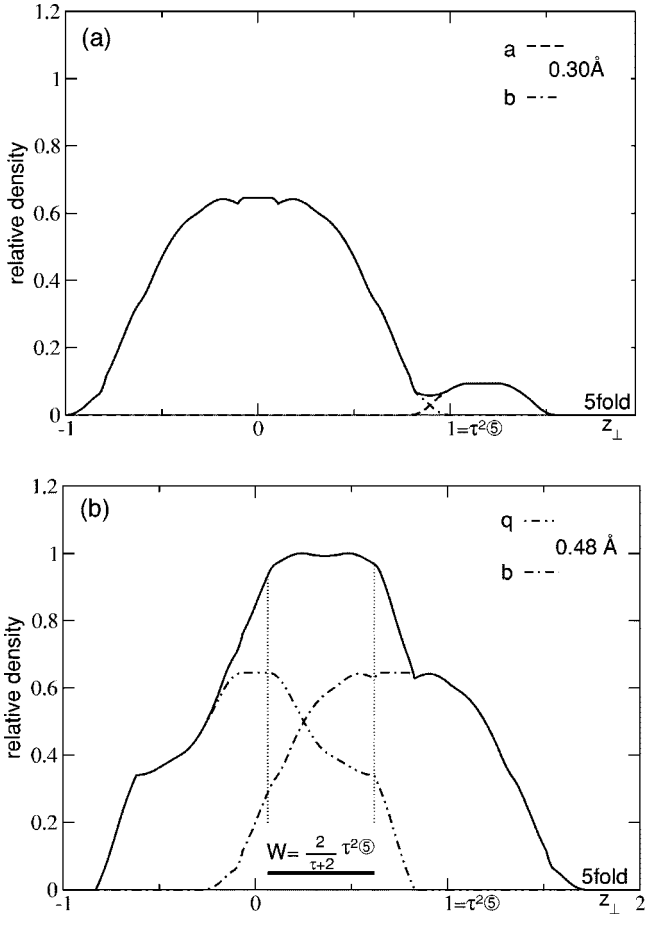


FIG. 6. Candidates for fivefold terminations of i-AlPdMn. The curves graph the density of layers along a fivefold axis $z_\perp$. The symbol ⑤ is the standard distance along a fivefold axis. (a) A pair of parallel *b* and *a* planes, a distance $\delta=0.30$ Å apart. The *b* curve is the density of atomic positions on *b* planes and the *a* curve the density on *a* planes, both functions of $z_\perp$. The solid curve is their sum. (b) A pair of parallel *q* and *b* planes, a distance $\delta=0.48$ Å apart. The *q* curve is the density of atomic positions on *q* planes and the *b* curve the density on *b* planes, both functions of $z_\perp$. The solid curve is their sum. Among the densest fivefold layers are $(q,b)$ pairs of planes a distance 0.48 Å apart. The support of the plateau of the solid curve of 0.48 Å $(q,b)$ layers defines the terminations and is the coding window of the Fibonacci sequence of terraces of terminations on fivefold surfaces. The height of the plateau is the density of fivefold terminations. The density graph of 0.78 Å layers has a lower maximum than the graph of 0.48 Å layers, and is not shown here. The 1.56 Å layer is also not shown, as we do not consider it a ''thin layer.'' For i-AlCuFe, the graphs are the same with slightly changed spacings; see Table II.

model of Boudard *et al.* with spherical windows,[23] used in Ref. 6, there are twofold planes denser than the densest fivefold or threefold planes even though experimental evidence indicates that the fivefold sputter-annealed surfaces are the most stable.[6]

In the light of this, and the fact that fivefold terminations are observed to consist of a pair of neighboring planes, we propose a modification to the Bravais rule to take into account close neighboring planes in the main symmetry directions (fivefold, twofold, and threefold) of the geometric model $\mathcal{M}$. In each of these directions the three shortest interplanar distances $(s,m,l)$ occur in the ratios $s:m:l=1:\tau:\tau^2$; see rows 2–4 of Table II. For the main symmetry directions we have examined the density graphs in coding space $\mathbb{E}_\perp$ of all single atomic planes and of all atomic layers containing two neighboring planes with the separations $\delta$ listed in Table II. Let us decide that layers of width $\delta=0.86$, 0.92, 1.48 or 1.56 Å cannot be regarded as thin layers forming a single termination. This is equivalent to defining a thin layer to be of thickness $\delta$ significantly smaller than 0.86 Å. We consider such thin layers as candidates for

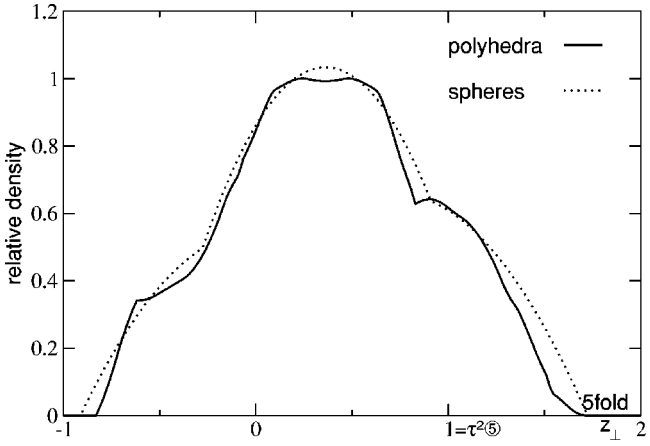


FIG. 7. If the windows in Fig. 5 are replaced by spheres of the same volume (Boudard's model) there is no pronounced plateau in the function $\rho(z_\perp)$ for the densest fivefold terminations. Compare the solid and dotted graphs.

TABLE II. $\mathcal{M}$ data of i-AlPdMn. Row 1: shortest interatomic distances parallel to the axis (min. IA distance). Rows 2–4: three shortest interplanar separations orthogonal to the axis (IP distances). Rows 5–7: other interplanar separations of neighboring planes. Row 8: $D_6$ module factor. Row 9: maximum absolute atomic density of planes. Row 10: maximum absolute atomic density of layerlike terminations. Row 11: maximum relative atomic density of layerlike terminations. The corresponding data for i-AlCuFe can be obtained by setting the standard length ⑤ to 4.465 Å.

| | fivefold | twofold | threefold |
|---|---|---|---|
| Min. IA distance | $\tau^{-1}⑤$ | $\tau^{-1}②$ | $\tau^{-1}③$ |
| | 2.82 Å | 2.96 Å | 2.57 Å |
| IP distances: $s$ | $\tau^{-3}⑤/(\tau+2)$ | $\tau^{-3}②/2$ | $\tau^{-4}③/3$ |
| | 0.30 Å | 0.57 Å | 0.20 Å |
| IP distances: $m=\tau s$ | 0.48 Å | 0.92 Å | 0.33 Å |
| IP distances: $l=\tau m$ | 0.78 Å | 1.48 Å | 0.53 Å |
| IP distance: $2m$ | | | 0.65 Å |
| IP distance: $\tau l$ | | | 0.86 Å |
| IP distance: $2l$ | 1.56 Å | | |
| $D_6$ module factor | $1/\sqrt{5}$ | 1/4 | 1/3 |
| Densest planes (abs.) | 0.086 $Å^{-2}$ | 0.101 $Å^{-2}$ | 0.066 $Å^{-2}$ |
| Densest layers (abs.) | 0.133 $Å^{-2}$ | 0.101 $Å^{-2}$ | 0.066 $Å^{-2}$ |
| Densest layers (rel.) | 1 | 0.76 | 0.50 |

the bulk terminations. We calculate the densities of $\delta$ layers orthogonal to a given symmetry axis $z_\parallel$ (taking the density of a thin layer to be the sum of the densities of the atomic planes within it). To do the calculation it is necessary to pass to the coding space $\mathbb{E}_\perp$ in order to find the window factor. But coding space also has the great advantage that the $\delta$ layers, which in physical space $\mathbb{E}_\parallel$ are distributed along the entire infinite length of the $z_\parallel$-axis with neighboring layers having widely different densities, are $*$-mapped to a finite interval of $z_\perp = z_\parallel^*$ in $\mathbb{E}_\perp$, and that within this interval the density of layers is a smooth function of position, $\rho(z_\perp)$, which can be graphed. The maximum of this graph determines the maximum possible density of a $\delta$ layer in the bulk. For a given axis $z_\parallel$, we compare the graphs of all possible $\delta$ layers and choose the one with the highest maximum. If a maximum density rule is valid, then the terminations orthogonal to the $z_\parallel$ axis should be the densest $\delta$ layers for this value of $\delta$. If the density graph for this $\delta$ has a plateau (i.e., a region of almost constant maximum density) the width of the support, $W$, of the plateau will determine the sequence of bulk terminations and hence the sequence of terraces that appear on the surface.

Comparing terminations orthogonal to different directions, we expect the more stable surfaces to correspond to the denser terminations, i.e., to the density function with the higher maximum. To test this we plot in coding space $\mathbb{E}_\perp$ the density graphs $\rho(z_\perp)$ of $\delta$-layers, determine the terminations of our model $\mathcal{M}$ in the fivefold, twofold, and threefold directions, and compare them with the experimental data.

The $z_\perp$ axis in each of the graphs in Figs. 6, 7, 9, and 10 is a fivefold, twofold, and threefold axis in coding space. A $\delta$ layer, specified in physical space $\mathbb{E}_\parallel$ by the point where its topmost plane meets the $z_\parallel$ axis, is represented by the *-map of this point on $z_\perp$. The ordinate in the graph is the relative density of the layer with respect to the densest fivefold termination in Fig. 6(b).

Comparing the density graphs of fivefold layers in Figs. 6(a) and 6(b) we conclude that indeed, as anticipated in Refs. 1 and 13, the densest fivefold layers of thickness significantly less than 1.56 Å are pairs of planes 0.48 Å apart as in Fig. 6(b). This agrees with experimental evidence.[1,13] Figure 6(b) graphs the atomic density $\rho(z_\perp)$ of $(q,b)$ pairs of planes as a function of position along a fivefold $z_\perp$ axis in coding space $\mathbb{E}_\perp$. It is close to its maximum along a clear plateau of width about $[2\tau^2/(\tau+2)]$ ⑤. The interval of this plateau (a ''window'' $W$) codes a Fibonacci sequence along a fivefold axis $z_\parallel$ in $\mathbb{E}_\parallel$ of short ($S$) and long ($L$) intervals: $S=(2\tau/(\tau+2))$ ⑤$=4.08$ Å (⑤ is 4.561 Å for i-AlPdMn) and $L=\tau S=6.60$ Å, in agreement with Ref. 9 and references cited there. A slightly longer interval codes a decorated Fibonacci sequence[1] that includes steps of height $\tau^{-1}S=2.52$ Å too, detected in Ref. 24.

On the fivefold surfaces of i-AlCuFe only short sequences of up to 6 terraces have been detected;[25] they seem Fibonacci-like, but with some defects. The step heights are $S=4.0$ Å and $L=6.2$ Å, in reasonable agreement with our predicted values $S=[2\tau/(\tau+2)]$ ⑤$=3.99$ Å (⑤ is 4.465 Å for i-AlCuFe) and $L=\tau S=6.46$ Å.

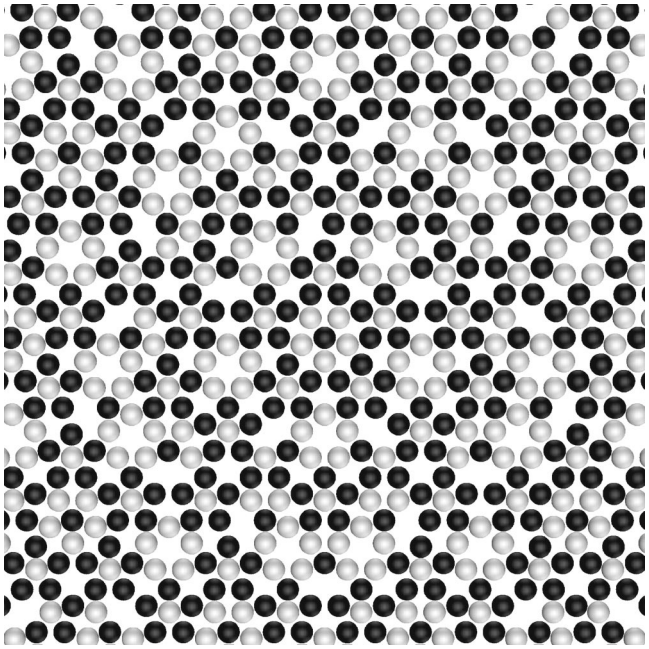

FIG. 8. A fivefold termination (rich in Al) consisting of a $(q,b)$ layer of two atomic planes 0.48 Å apart. The atoms are represented as balls, the size of Al atoms. The black balls are those in the surface $q$ plane and the white balls those in the $b$ plane, 0.48 Å below the surface. Compare the distance between the planes in a layer with the shortest interatomic distances in row 1 of Table II.

Figure 7 shows that there is not such a clearly defined plateau as in Fig. 6(b) when the windows of the model $\mathcal{M}$ (Fig. 5) are replaced by the spheres of the same volumes used by Boudard[7] (and there called ''atomic surfaces'').

As the $(q,b)$ layers (modeled in Fig. 8) there are also $(b,q)$ layers in $\mathcal{M}$ whose density graph is the mirror image of Fig. 6(b) and codes another Fibonacci sequence of equally dense layers. These $(b,q)$ layers are *not* seen as surface terminations. The planes observed on the surface can be identified as type $q$ by the presence (in some terraces of a surface Fibonacci sequence) of a local configuration called a ''ring.''[1] This preference of $(q,b)$ layers to become the terminations can perhaps be understood from the densities of the parallel planes next above and below the layers: above a $(q,b)$ layer there is a low-density plane and below a high-density plane; for the mirror-image $(b,q)$ layer the neighboring planes are mirrored too.

The densest twofold layers are single planes, seen by comparing the graphs in Figs. 9(a) and 9(b). In Fig. 9(b) we can identify a not very sharply defined plateau of width about ②/2 that defines the twofold terminations. A window of this width on a twofold axis in $\mathbb{E}_\perp$ encodes a Fibonacci sequence of terminations along a twofold axis of $\mathbb{E}_\parallel$ with $S=(\tau^2/2)$ ②$=0.63$ nm, $L=\tau S=1.02$ nm. These intervals are close to the steps between terraces (0.62 nm and 0.95 nm) in Fig. 3(c). Increasing the width of the window by a factor $\tau^2$ would include less dense planes to reduce the lengths of intervals in the Fibonacci sequence by $\tau^{-2}$, making them 0.24 nm and 0.38 nm corresponding to the measured depths 0.24 nm and 0.36 nm of the depressions in the

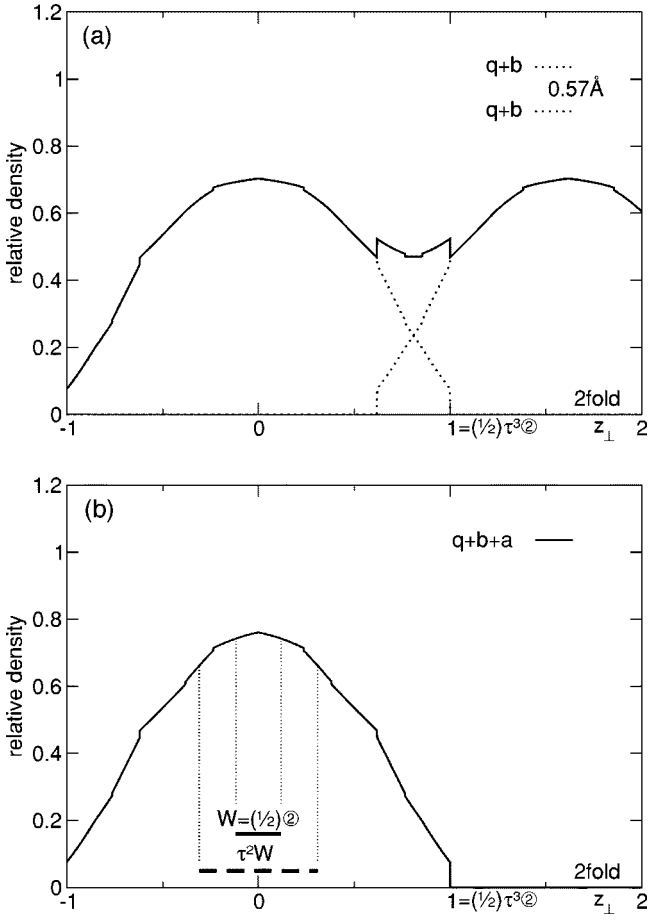


FIG. 9. Candidates for twofold terminations of i-AlPdMn. The curves graph the density of layers along a twofold axis, $z_\perp$. The symbol ② is the standard distance along a twofold axis, ② $=2$ ⑤$/\sqrt{\tau+2}$. (a) A pair of the parallel planes, each containing *b*- and *q*-atomic positions, a distance 0.57 Å apart. (b) A single plane containing *b*-, *q*-, and *a*-atomic positions. The curve in (b) has its maximum marginally higher than in the curve in (a), so the densest twofold layers are single planes, which contain atomic positions of types *q*, *b*, and *a*. We do not consider the 0.92 Å or 1.48 Å layers as "thin layers." For i-AlCuFe, the graphs are the same with slightly changed spacings; see Table II.

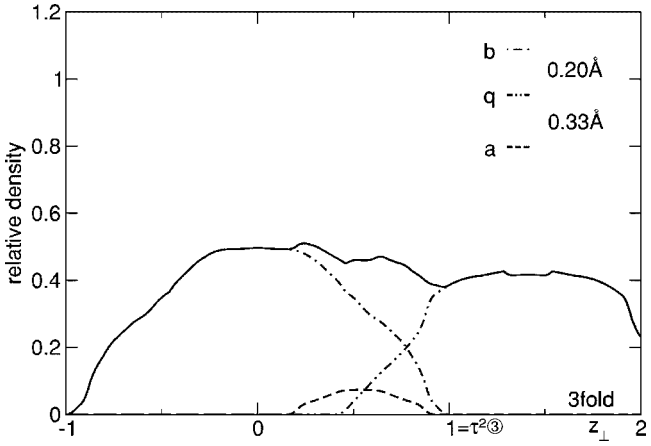


FIG. 10. Graph of the density of $(b,q,a)$ triples of threefold planes (in $\mathbb{E}_\perp$ orthogonal to a threefold axis $z_\perp$) of i-AlPdMn with spacings: *b* plane, 0.20 Å, *q* plane, 0.33 Å, *a* plane. The symbol ③ is the standard distance in $\mathbb{E}_\perp$ along the threefold axis, ③ $=\sqrt{3}$ ⑤$/\sqrt{\tau+2}$. The plateau in the graph of the combined density defines the terminations, its height giving their density. The density graph of 0.65 Å layers (not shown) has a very low maximum. We do not consider the 0.86 Å layer a "thin layer." For i-AlCuFe, the graphs are the same with slightly changed spacings; see Table II.

big terraces in Fig. 3 (c). These depressions can therefore be interpreted as less dense, hence lower probability, terraces coexisting with the denser, high probability terraces and giving them a rougher character.

One can show from the density graphs in $\mathbb{E}_\perp$ that the densest threefold layers are $(b,q,a)$ and $(a,q,b)$ triples of planes with distances 0.20 Å between the *b* and *q* planes and 0.33 Å between the *q* and *a* planes. The graph of the densities of the $(b,q,a)$ layers as a function of position in coding space is shown in Fig. 10 and has a wide plateaulike area around its maximum. This is in qualitative agreement with the medium scale terraces that spread over an area of about $1000\times1000$ nm$^2$ on the threefold surface shown in Fig. 4. Unlike the fivefold case, parts of this plateau correspond to single *b* planes or *q* planes, where the densities of the other planes drop to zero. As the $(b,q,a)$ layers there are also $(a,q,b)$ layers in $\mathcal{M}$ whose density graph is the mirror image of Fig. 10. A height profile along a line, with step heights, like that for the twofold surface in Fig 3(c), has not been determined for the threefold surface.

The relative maximum densities of the fivefold, twofold, and threefold terminations can be read off from the graphs shown in Figs. 6(b), 9(b) and 10, and we list them in row 11 of Table II. They are in the order fivefold, twofold, and threefold. Row 10 of Table II gives the absolute maximum densities of fivefold, twofold, and threefold terminations for the model $\mathcal{M}$ of i-AlPdMn. The corresponding data for i-AlCuFe can be obtained by setting the standard length ⑤ to 4.465 Å.

## IV. CONCLUSIONS

We expect that, with our modified definition of termination as a thin layer of stacked atoms and not just a single atomic plane, the Bravais rule that the densest bulk terminations correspond to the most stable surfaces may be widely applicable to quasicrystals. A significant feature of this approach is that measurable properties of coding space predict observable properties of physical surfaces. The shape of the density graph of a layer in coding space determines (1) the relative stability of the surface (by the height of its maximum) and (2) the texture of the surface (by the breadth of its maximum). If the maximum of the function has the form of a flat plateau, as for the fivefold and threefold layers in Figs. 6(b) and 10, then the surfaces have a pronounced terracelike character, as in Figs. 1 and 4. The terraces correspond to bulk layers of almost equal density and for that reason are equally probable as surfaces and are of almost equal size. On the other hand, the sharper peak for the twofold layers in Fig. 9(b) determines the more fragmented appearance of the twofold surface seen in Figs. 2 and 3. Terraces of distinctly different areas correspond to bulk layers of different densities that are not equally probable: on relatively large (more

probable) terraces smaller (less probable) terraces appear as holes.

Measurements of the fivefold surfaces of i-AlCuFe also support our modified density rule, and we expect it to apply to all icosahedral quasicrystals. There are preliminary indications that a related rule applies to decagonal quasicrystals,[16] but in the case of d-AlCuCo the candidate for a termination is a ''broad layer'' (see Sec. V) rather than a thin layer of the kind described in Sec. III.

## V. FUTURE DIRECTIONS

A feature of the surface of i-AlPdMn not accounted for by our layer analysis is that not all types of maximally dense layers appear as surfaces: for example, $(q,b)$ layers are seen in fivefold surfaces but equally dense $(b,q)$ layers are not. One possibility is that the densities of the planes above and below the layer may influence whether it appears as a surface. If one chose to define a termination incorporating the neighboring planes too, one could introduce a broad layer as a bundle of high-density thin layers. This is done in Ref. 16. For example, a fivefold termination can be considered to be a broad layer consisting of a $(q,b)$ layer and a $(b,q)$ layer, each with $\delta=0.48$ Å. So such a broad layer contains four planes with spacings: $q$ plane, 0.48 Å, $b$ plane, 1.56 Å, $b$ plane, 0.48 Å, $q$ plane. It can be shown[16] that the density graph of such a configuration also supports the appearance of a Fibonacci sequence of terraces on the fivefold surfaces of i-AlPdMn. In fact most $(q,b)$ thin layer terminations occur within such $(q,b,b,q)$ broad layer terminations.[16] Similarly, we may replace a single dense twofold atomic plane by a layer of four atomic planes[16] with spacings: $abq$ plane, 1.48 Å, $bq$ plane, 0.92 Å, $bq$ plane, 1.48 Å, $abq$ plane. For these broad layer twofold terminations the peak becomes a perfectly flat plateau, and the appearance of the small terraces within the big ones must be explained by the comparatively larger distances between the atomic planes in a terminating layer.[16]

On the experimental evidence to date, in the case of i-AlPdMn, it is not possible to say whether thin layer or broad layer terminations best model the physical surfaces,[16] but both share the feature that densities of layers of more than one atomic plane are used to determine the positions of the bulk terminations.

*Author to whom correspondence should be addressed. FAX: +49-7071-29-5604. Email address: zorka.papadopolos@uni-tuebingen.de

[1] Z. Papadopolos, G. Kasner, J. Ledieu, E.J. Cox, N.V. Richardson, Q. Chen, R.D. Diehl, T.A. Lograsso, A.R. Ross, and R. McGrath, Phys. Rev. B **66**, 184207 (2002).

[2] A. Bravais, Etudes Cristallographiques, Premiére partie: du Cristal Considéré Comme un Simple Assemblage de Points (presented 26.02.1849), J.E. Polytech. XXXIV Cahier, pp. 13-25, in Etudes Crystallographiques, Gauthier-Villars, Paris, 1866.

[3] J.D.H. Donnay and D. Harker, Am. Mineral. **22**, 446 (1937).

[4] T. Aste and D. Weaire, in *The Pursuit of Perfect Packing* (Institute of Physics, Bristol and Philadelphia, 2000), p. 84.

[5] J.L. Aragón, F. Dávila, and A. Gómez, Phys. Rev. B **51**, 857 (1995).

[6] Z. Shen, W. Raberg, M. Heinzig, C.J. Jenks, V. Fournée, M.A. Van Hove, T.A. Lograsso, D. Delaney, T. Cai, P.C. Canfield, I.R. Fisher, A.I. Goldman, M.J. Kramer, and P.A. Thiel, Surf. Sci. **450**, 1 (2000).

[7] M. Boudard, M. de Boissieu, C. Janot, G. Heger, C. Beeli, H.-U. Nissen, H. Vincent, R. Ibberson, M. Audier, and J.M. Dubois, J. Phys.: Condens. Matter **4**, 10149 (1992).

[8] Z. Papadopolos, P. Kramer, and W. Liebermeister, in *Proceedings of the International Conference on Aperiodic Crystals, Aperiodic 1997*, edited by M. de Boissieu, J.-L. Verger-Gaugry, and R. Currant (World Scientific, Singapore, 1998), p. 17.

[9] G. Kasner, Z. Papadopolos, P. Kramer, and D.E. Bürgler, Phys. Rev. B **60**, 3899 (1999).

[10] Z. Papadopolos, P. Kramer, G. Kasner, and D.E. Bürgler, in *Quasicrystals*, edited by J. M. Dubois, P. A. Thiel, A.-P. Tsai, and K. Urban, Mater. Res. Soc. Symp. Proc. 553 (Materials Research Society, Warrendale, PA, 1999), p. 231.

[11] D.S. Rokhsar, N.D. Mermin, and D.C. Wright, Phys. Rev. B **35**, 5487 (1987).

[12] See, www. Webelements. com

[13] M. Gierer, M.A. Van Hove, A.I. Goldman, Z. Shen, S.-L. Chang, C.J. Jenks, C.-M. Zhang, and P.A. Thiel, Phys. Rev. Lett. **78**, 467 (1997); M. Gierer, M.A. Van Hove, A.I. Goldman, Z. Shen, S.-L. Chang, P.J. Pinhero, C.J. Jenks, J.W. Anderegg, C.-M. Zhang, and P.A. Thiel, Phys. Rev. B **57**, 7628 (1998).

[14] A.R. Kortan, R.S. Becker, F.A. Thiel, and H.S. Chen, Phys. Rev. Lett. **64**, 200 (1990).

[15] S.E. Burkov, Phys. Rev. B **47**, 12 325 (1993).

[16] Z. Papadopolos, G. Kasner, and A. R. Kortan (unpublished).

[17] C. Beeli, T. Gödecke, and R. Lück, Philos. Mag. Lett. **78**, 339 (1998).

[18] L. Barbier, D. Le Floc'h, Y. Calvayrac, and D. Gratias, Phys. Rev. Lett. **88**, 085506 (2002).

[19] V. Elser, Philos. Mag. B **73**, 641 (1996).

[20] A. Katz and D. Gratias, in *Proceedings of the Fifth International Conference on Quasicrystals*, edited by C. Janot and R. Mosseri (World Scientific, Singapore, 1995), p. 164.

[21] R. V. Moody, in *The Mathematics of Long-Range Aperiodic Order*, edited by R. V. Moody (Kluwer, Dordrecht, 1997), pp. 403–441.

[22] P. Pleasants, in *Covering of Discrete Quasiperiodic Sets: Theory and Applications to Quasicrystals*, Springer Tracts in Modern Physics Vol. 180, edited by P. Kramer and Z. Papadopolos (Springer, Berlin, 2002), p. 185.

[23] The Boudard model is defined by three windows denoted by $W_{n_0}$, $W_{n_1}$, and $W_{bc_1}$, see Fig. 1(b) in Ref. 6 where windows are called ''atomic surfaces.'' These windows are balls with volumes equal to the volumes of $W_q$, $W_b$, and $W_a$ in Fig. 5 of the present paper.

[24] Z. Shen, C.R. Stoldt, C.J. Jenks, T.A. Lograsso, and P.A. Thiel, Phys. Rev. B **60**, 14 688 (1999).

[25] T. Cai, F. Shi, Z. Shen, M. Gierer, A.I. Goldman, M.J. Kramer, C.J. Jenks, T.A. Lograsso, D.W. Delaney, P.A. Thiel, and M.A. Van Hove, Surf. Sci. **495**, 19 (2001).